

Long Run Evolution, Path Dependence and Global Properties of Dynamic Games: A Tutorial

Gian-Italo Bischi

Istituto di Scienze Economiche, University of Urbino,

I-61029 Urbino, Italy

e-mail address: bischi@econ.uniurb.it

and

Michael Kopel

Department of Managerial Economics and Industrial Organization

University of Technology, Theresianumgasse 27, A-1040 Vienna, Austria

e-mail address: kopel@mail.ibab.tuwien.ac.at

SUMMARY. In this paper we consider dynamic game-theoretic models, where boundedly rational players use simple decision rules to determine their actions over time. The adaptive process which captures the interaction of the players' decisions is the main objective of our study. In many situations this process is characterized by multistability, where e.g. multiple stable (Nash) equilibria emerge as possible long run outcomes. When such coexistence occurs, the selected equilibrium becomes path-dependent, and a thorough knowledge of the basins and their structure becomes crucial for the researcher to be able to predict which one of the multiple equilibria is more likely to be observed in situations described by the game. We demonstrate that, despite the fact that the long run dynamics of the adaptive process might be rather simple, the basins of the attracting sets might have quite complicated structure. In this paper we show that the complexity of basins can be explained on the basis of the global properties of the dynamical system, and we introduce the main tools – critical sets and basin boundaries – which enable the model builder to analyze the extent of the basins and their changes as structural parameters of the model are changed. The main point is that one has to study the global properties of the system, and not restrict the investigation to the local dynamics around the attracting sets.

1 Introduction

For quite a long time the standard approach in game theory textbooks treated the question of outcomes in static games. Static in this context refers to the fact that players meet only once and by some kind of process of introspection simultaneously and immediately choose strategies which correspond to a (Nash) equilibrium. Players were assumed to be fully rational, i.e. they know everything about the game they are playing (and also know that the same is true for the other players). However, in real world situations complexities and difficulties arise, e.g. the limited ability of agents to compute optimal solutions, the difficulty to foresee all contingencies in the future and prohibitive costs to calculate and implement an optimal plan of action. Accordingly, due to these restrictions which agents in the real world have to face, they only behave boundedly rational. In the more recent literature, dynamic situations are considered, where players interact with each other repeatedly over time and often choose their actions or strategies by trial and error methods that require less information and a lower degree of rationality of the players. It is assumed that agents behave adaptively and adjust their strategies to changes in their environment; see e.g. Binmore [5], Weibull [32], Hofbauer and Sigmund [20], Fudenberg and Levine [18]. Convergence to a Nash equilibrium of a dynamic game played by boundedly rational agents means that this equilibrium is not the result of some fixed point argument (and is assumed to be reached by fully rational players in one shot), but instead emerges in the long run as the result of an adaptive process. This “evolutionary approach” to Nash equilibrium reinforces its meaning as a real world outcome. This becomes even more important as observations in the field of experimental economics provides evidence that players find their way to an equilibrium of a game by using trial-and-error methods (see e.g. Binmore, [6]).

In this paper we focus on this line of research and consider situations where boundedly rational agents interact repeatedly. The dynamic process by which players adapt their choices over time can be formally described as follows. At each discrete time period $t = 0, 1, 2, \dots$, the n players choose their actions by using some (more or less sophisticated) decision rules, based on the information about past behavior. Players’ actions are represented by real numbers, $x_1(t), \dots, x_n(t)$, i.e. a point in a n -dimensional strategy space $S \in \mathbb{R}^n$. The adjustment process, which governs the evolution of the game can then be expressed in the form of a discrete dynamical system defined in $S \subseteq \mathbb{R}^n$. Given an initial choice of the players (the initial condition) $\mathbf{x}(0) \in S$, the sequence of actions $\mathbf{x}(t)$, $t \in \mathbb{N}$, is obtained *inductively* by the iteration of a map $T : S \rightarrow S$ defined by

$$\mathbf{x}' = T(\mathbf{x}) \tag{1}$$

where $'$ denotes the unit-time advancement operator. That is, if the right hand side variables represent the players’ actions at time period t , then the left hand side represents the set

of actions at time $(t + 1)$. As a classical example, we mention the Cournot tâtonnement process, by which players adjust their production sequences in a quantity-setting oligopoly game (see Cournot, [15]). In this game it is assumed that in each period every player chooses its own production strategy as a best response to the choices of the competitors in the previous period. The map T can then be derived on the basis of the players' best replies. Starting from an *initial condition* $\mathbf{x}_0 \in S$, the repeated application (*iteration*) of the map T uniquely defines a *trajectory of players' actions*

$$\tau(\mathbf{x}_0) = \{\mathbf{x}(t) = T^t(\mathbf{x}_0), t = 0, 1, 2, \dots\}, \quad (2)$$

where T^0 is the identity map and $T^t = T(T^{t-1})$. The main goal is to study the asymptotic evolution of these trajectories and how it is influenced by the starting conditions of the game (initial values of actions) and the values of some structural parameters of this game. The asymptotic properties of a trajectory as $t \rightarrow \infty$ represent the long run outcome of the game, which may be convergence to a Nash equilibrium, a bounded cyclic or chaotic motion around an (unstable) Nash equilibrium, or an irreversible departure from it. In some cases, trajectories may even exit the strategy space, i.e. diverging trajectories may be obtained.

The insight that a dynamic process defined by the iterated map (1) may converge to a given steady state (or equilibrium), but also may lead to more complex behavior, has been rather influential. In a pioneering paper, Rand [27] has shown that quite complex dynamics with periodic and chaotic trajectories may characterize the long run evolution of dynamic (duopoly) games. In the following years other authors have given examples of economically interesting dynamic games, showing complex dynamics; see, e.g. Dana and Montrucchio [16], Van Witteloostuijn and Van Lier [31], Puu [25], [26], Kopel [21], Agiza et al. [2], Bischi et al. [10], Rosser [29]. In these papers it is shown that trajectories of actions might never settle to any steady state and in the long run exhibit bounded dynamics which may be periodic, quasi-periodic or even chaotic. Divergence from an equilibrium in this context means that the Nash equilibrium is not really relevant because it cannot be endogenously learned by boundedly rational agents.

A rather different problem which often arises in the study of dynamic games concerns the coexistence of several equilibria, each with its own basin of attraction. In this case, a problem of equilibrium selection arises (see Van Huyck et al. [30], Bischi and Kopel [7]), and a mechanism is required that allows to make predictions which of the multiple equilibria (or other attracting sets) will be more likely observed in situations described by the game. One approach to select among the equilibria is to use stability arguments. The idea behind this approach is that an equilibrium point is a convention that arises among players interacting repeatedly. As unstable equilibria will not be the result of such an evolutionary process, only stable equilibria have to be considered. If such a stability argument selects a single

equilibrium, we can abstract from the process itself with its undesirable dependence on historical accident. However, often many equilibria survive this refinement, and a situation of strategic uncertainty prevails. In such situations of *multistability*, the selected equilibrium is path-dependent and the choices of the initial actions (the initial condition) are of crucial importance. In other situations, stable Nash equilibria might even coexist with other kinds of attractors and the boundedly rational players may in the long run learn to play Nash equilibrium strategies or they may continue to play a different set of strategies that are not part of any equilibrium selected by fully rational players.

Such situations of multistability quite naturally lead to the study of the basins of attraction, which requires a global analysis of the dynamical system (1). In fact, a local stability analysis, based on the linear approximation of the dynamical system around the steady states, is not enough to characterize the structure of the basins and their qualitative changes. Local stability means that the game converges to a particular attracting set in the long run, provided that the initial strategies are sufficiently close to it. On the other hand, interesting phenomena may occur when the game starts far away from an equilibrium (or, in general, from an attracting set), since global dynamic properties may influence the time path due, for example, to overreactions of the agents when their strategies are very far from all the equilibria. However, this question and, related to it, the study of the complex structure of the basins has been rather neglected in the economics and game theory literature.

An investigation of global bifurcations that change the qualitative structure of the basins is particularly challenging in the case of discrete time dynamical systems governed by the iteration of noninvertible maps. Indeed, in this case the basins may have complicated topological structures, since they may be multiply-connected or non-connected sets, often formed by the union of infinitely many disjoint portions. With the help of recent results on basin bifurcations in noninvertible maps, mainly based on the method of critical sets (see e.g. Mira et al. [23], [24], Bischi and Kopel [7]), insights into the structure of the basins and into the creation of complex basin boundaries can be obtained. As some parameter is varied, such changes in the structure can be characterized by global bifurcations: they are the consequence of *contact bifurcations*, i.e. due to contacts between critical sets and invariant sets (such as fixed points or cycles or their stable sets). For two-dimensional maps, such kinds of bifurcations can be very rarely studied by analytical methods, since the equations of such singularities are not known in general. Hence these global bifurcations are mainly studied by geometrical and numerical methods. For recent applications to models of economic and financial systems, see e.g. Bischi et al. [9], [10], Agliari et al. [3], Puu [26], Bischi and Kopel [7].

Summarizing, we may say that in the literature on dynamic games two different routes to complexity have been studied. The first one is related to the complexity of the attracting sets

which characterize the long run evolution of the dynamic process and describe the evolution of players' actions over time. The second one focuses on the complexity of the boundaries which separate the basins when several coexisting attractors are present. It is important to realize that these two different kinds of complexity are *not related*. Very complex attractors may have simple basin boundaries, whereas boundaries which separate the basins of simple attractors, such as coexisting stable equilibria, may have very complex structure. Since we feel that for game theoretic considerations the second line of research is more important, we will mainly focus on the global analysis of dynamic games, the study of the basins of attraction of long run outcomes, the basin boundaries in situations of multistability, and the corresponding changes when structural parameters of the games are changed.

The paper is organized as follows. In Section 2, we briefly review some important definitions and concepts from the theory of dynamical systems. In section 3 we consider one-dimensional maps, and illustrate how global bifurcations give rise to non-connected basins of attracting sets. We then consider two-dimensional examples in section 4. We take economic applications of dynamic games, and show that complicated structures of the basins may emerge, although the long run dynamics of these games are rather simple. Section 5 concludes.

2 Some Definitions

In this section we recall some definitions concerning discrete dynamical systems represented by iterated maps of the form (1). The point \mathbf{x}' is called the *rank-1 image* of \mathbf{x} . A point \mathbf{x} such that $T(\mathbf{x}) = \mathbf{x}'$ is called a *rank-1 preimage* of \mathbf{x}' . The point $\mathbf{x}(t) = T^t(\mathbf{x})$, $t \in \mathbb{N}$, is called image of rank- t of the point \mathbf{x} , where T^0 is identified with the identity map and $T^t(\cdot) = T(T^{t-1}(\cdot))$. A point \mathbf{x} such that $T^t(\mathbf{x}) = \mathbf{y}$ is called rank- t preimage of \mathbf{y} .

A set $A \subset \mathbb{R}^n$ is *trapping* if it is mapped into itself, $T(A) \subseteq A$, i.e. if $\mathbf{x} \in A$ then $T(\mathbf{x}) \in A$. A trapping set is *invariant* if it is mapped onto itself: $T(A) = A$, i.e. all the points of A are images of points of A . A closed invariant set A is an attractor if it is *asymptotically stable*, i.e. if a neighborhood U of A exists such that $T(U) \subseteq U$ and $T^t(\mathbf{x}) \rightarrow A$ as $t \rightarrow +\infty$ for each $\mathbf{x} \in U$.

The *Basin of an attractor* A is the set of all points that generate trajectories converging to A

$$\mathcal{B}(A) = \{\mathbf{x} | T^t(\mathbf{x}) \rightarrow A \text{ as } t \rightarrow +\infty\}. \quad (3)$$

Starting from the definition of stability, let $U(A)$ be a neighborhood of an attractor A whose points converge to A . Of course $U(A) \subseteq \mathcal{B}(A)$, but note that also the points of the phase space which are mapped inside U after a finite number of iterations belong to $\mathcal{B}(A)$. Hence,

the *total basin of A* (or briefly the basin of A) is given by

$$\mathcal{B}(A) = \bigcup_{n=0}^{\infty} T^{-n}(U(A)), \quad (4)$$

where $T^{-1}(\mathbf{x})$ represents the set of the rank-1 preimages of \mathbf{x} (i.e. the points mapped into x by T), and $T^{-n}(x)$ represents the set of the rank- n preimages of x (i.e. the points mapped into x after n applications of T).

A map T is said to be noninvertible (or “many-to-one”), if distinct points $\mathbf{x} \neq \mathbf{y}$ exist which have the same image, $T(\mathbf{x}) = T(\mathbf{y}) = \mathbf{x}'$. This can be equivalently stated by saying that points exist which have several rank-1 preimages, i.e. the inverse relation $\mathbf{x} = T^{-1}(\mathbf{x}')$ may be multi-valued. Geometrically, the action of a noninvertible map T can be described by saying that it “folds and pleats” the plane, so that two distinct points are mapped into the same point. Equivalently, we could also say that several inverses are defined, and these inverses “unfold” the plane. For a noninvertible map T , the space \mathbb{R}^n can be subdivided into regions Z_k , $k \geq 0$, whose points have k distinct rank-1 preimages. Generally, as the point \mathbf{x}' varies in \mathbb{R}^n , pairs of preimages appear or disappear as this point crosses the boundaries which separate different regions. Hence, such boundaries are characterized by the presence of at least two coincident (or merging) preimages. This leads to the definition of the critical sets, one of the distinguishing features of noninvertible maps (Mira et al., [24]): The *critical set CS* of a continuous map T is defined as the locus of points having at least two coincident *rank* – 1 preimages, located on a set CS_{-1} called *set of merging preimages*. The critical set CS is the n -dimensional generalization of the notion of critical value (when it is a local minimum or maximum value) of a one-dimensional map¹, and of the notion of *critical curve LC* of a noninvertible two-dimensional map (from the French “Ligne Critique”). The set CS_{-1} is the generalization of the notion of critical point (when it is a local extremum point) of a one-dimensional map, and of the fold curve LC_{-1} of a two-dimensional noninvertible map. The critical set CS is generally formed by $(n - 1)$ -dimensional hypersurfaces of \mathbb{R}^n , and portions of CS separate regions Z_k of the phase space characterized by a different number of *rank* – 1 preimages, for example Z_k and Z_{k+2} (this is the standard occurrence).

As an illustration, we consider the well-known one-dimensional logistic map (fig. 1a)

$$x' = f(x) = \mu x(1 - x). \quad (5)$$

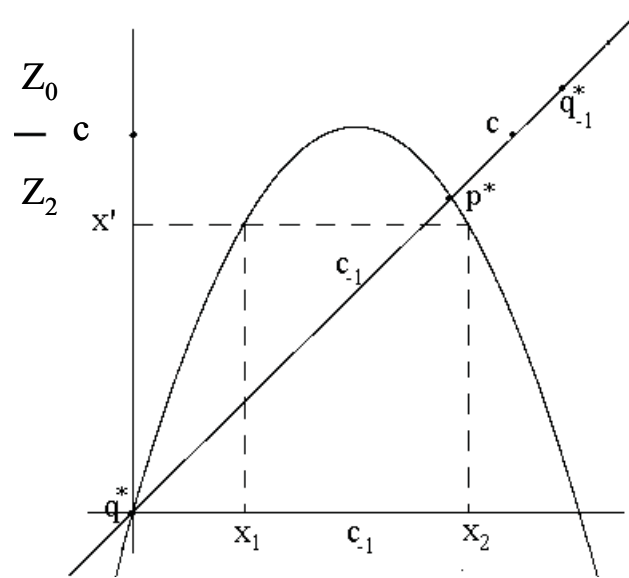
This map has a unique critical point $c = \mu/4$, which separates the real line into the two subsets: $Z_0 = (c, +\infty)$, where no inverses are defined, and $Z_2 = (-\infty, c)$, whose points have

¹This terminology, and notation, originates from the notion of critical points as it is used in the classical works of Julia and Fatou.

two rank-1 preimages. These preimages can be computed by the two inverses

$$x_1 = f_1^{-1}(x') = \frac{1}{2} - \frac{\sqrt{\mu(\mu - 4x')}}{2\mu}; \quad x_2 = f_2^{-1}(x') = \frac{1}{2} + \frac{\sqrt{\mu(\mu - 4x')}}{2\mu}. \quad (6)$$

If $x' \in Z_2$, its two rank-1 preimages, computed according to (6), are located symmetrically with respect to the point $c_{-1} = 1/2 = f_1^{-1}(\mu/4) = f_2^{-1}(\mu/4)$. Hence, c_{-1} is the point where the two merging preimages of c are located. The map f folds the real line, the two inverses unfold it (fig. 1b). As the map (5) is differentiable, at c_{-1} the first derivative vanishes. However, note that in general a critical point may even be a point where the map is not differentiable. This happens for continuous piecewise differentiable maps such as the well known tent map or other piecewise linear maps. In these maps critical points are located at the kinks where two branches with slopes of opposite sign join and local maxima and minima are located.



(a)

Figure 1a

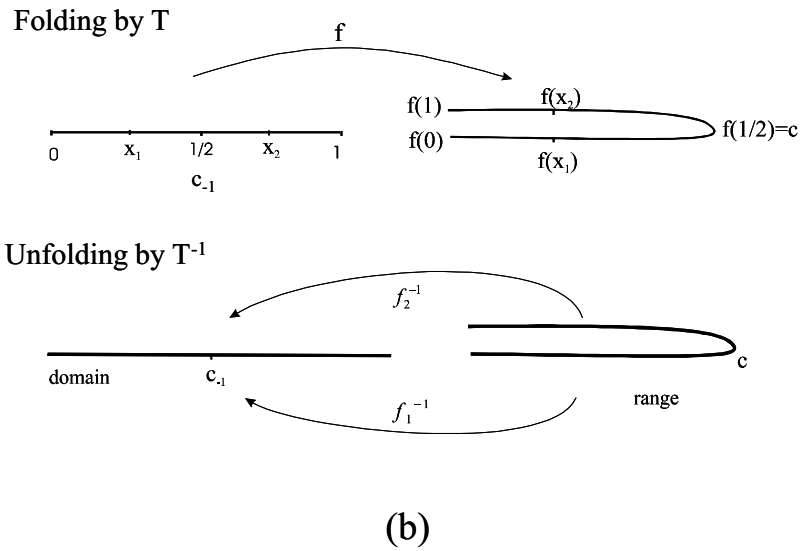


Figure 1b

Analogously, for a two-dimensional continuous map the set LC_{-1} is included in the set where $\det DT(x, y)$ changes sign, since T is locally an orientation preserving map near points (x, y) such that $\det DT(x, y) > 0$ and orientation reversing if $\det DT(x, y) < 0$. An intuitive visualization in \mathbb{R}^2 is given in fig. 2. Also in this case, if the map is continuously differentiable, the points of LC_{-1} necessarily belong to the set where the Jacobian determinant vanishes, and $LC = T(LC_{-1})$ constitutes the boundary lines which separates regions Z_k characterized by a different number of preimages.

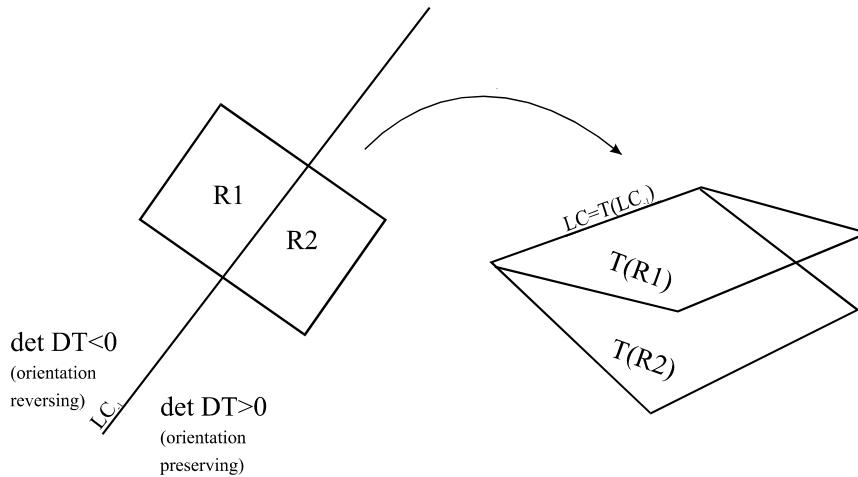


Figure 2

In order to give a geometrical interpretation of the action of a multi-valued inverse relation T^{-1} , it is useful to consider a region Z_k as the superposition of k sheets, each associated with a different inverse. Such a representation is known as *Riemann foliation* of the plane (see e.g. Mira et al., [24]). Different sheets are connected by folds joining two sheets, and the projections of such folds on the phase plane are arcs of LC . This is shown in the qualitative sketch of fig. 3, where the case of a $Z_0 - Z_2$ noninvertible map is considered. This graphical representation of the unfolding action of the inverses gives an intuitive idea of the mechanism which causes the creation of non-connected basins for noninvertible maps of the plane.

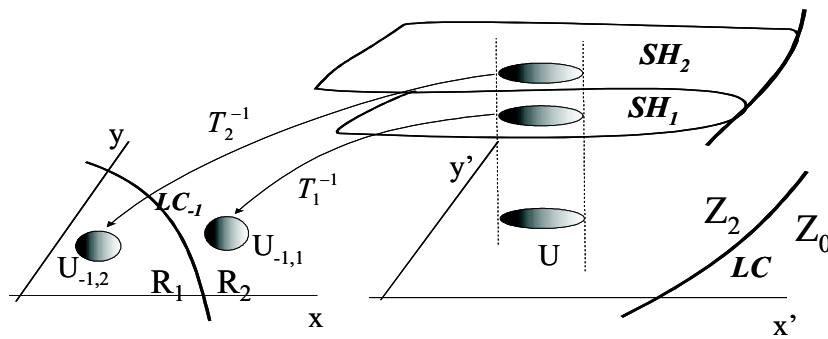


Figure 3

From the definition given above for the n -dimensional case, it is clear that the relation $CS = T(CS_{-1})$ holds, and the points of CS_{-1} , in which the map is continuously differentiable, are necessarily points where the Jacobian determinant vanishes. In fact, in any neighborhood of a point of CS_{-1} there are at least two distinct points which are mapped by T in the same point. Accordingly, the map is not locally invertible in points of CS_{-1} .

3 One-Dimensional Dynamics

In this section, we start with continuous, noninvertible and one-dimensional maps, and we illustrate how non-connected basins of attraction arise. Furthermore, we show how the global bifurcations that cause their qualitative changes can be described in terms of contacts between critical points and the basins' boundaries.

Let us first take a look at iterated invertible maps though. If $f : I \rightarrow I$ is a continuous and increasing function, then the only invariant sets are the fixed points. When many fixed points exist, say $x_1^* < x_2^* < \dots < x_k^*$, they are alternatingly stable and unstable: the unstable fixed points are the boundaries that separate the basins of the stable ones. Starting from an initial condition where the graph of f is above the diagonal, i.e. $f(x_0) > x_0$, the generated

trajectory is an increasing sequence converging to the stable fixed point on the right. On the other hand, starting from an initial condition such that $f(x_0) < x_0$, the trajectory is a decreasing sequence converging to the fixed point on the left (see fig. 4a, where p^* is a stable fixed point, and its basin is bounded by two unstable fixed points q^* and r^* , where $q^* < p^*$ and $r^* > p^*$). If $f : I \rightarrow I$ is a continuous and decreasing map, the only possible invariant sets are one fixed point and cycles of period 2. Periodic points of the cycles of period 2 are located around the fixed point, the unstable ones being boundaries of the basins of the stable ones (see fig. 4b, where a stable fixed point x^* exists, and its basin is bounded by the periodic points α_1, α_2 of an unstable cycle of period 2).

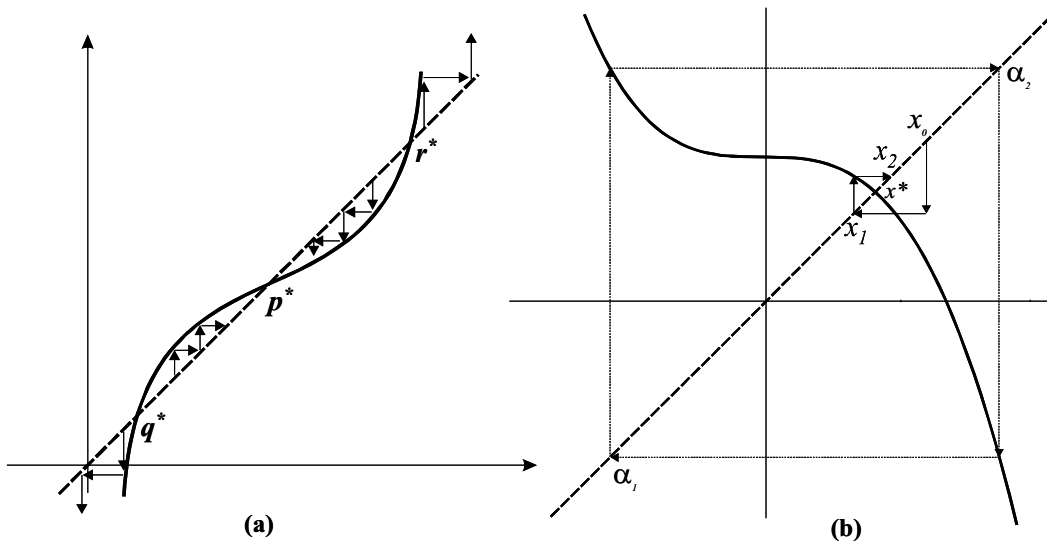


Figure 4

In general, in the case of one-dimensional invertible maps the only kinds of attractors are fixed points and cycles of period two. In the first case, the basin is an open interval which includes the fixed point, and in the second case, the basin is the union of two open intervals, each one including an attracting periodic point.

Obviously, if the map is invertible, the basins of the attracting sets are simple. This not true if the map is noninvertible. In this case the structure of a basin may be very complicated. Non-connected portions of the basins may be created, given by open intervals that do not include any point of the related attractor. As a first example, let us consider the logistic map (5), a noninvertible $Z_0 - Z_2$ map whose graph is represented again in fig. 5. For $\mu < 4$ every initial condition $x_0 \in (0, 1)$ generates bounded sequences, converging to a unique attractor A (which may be the fixed point $x^* = (\mu - 1) / \mu$ or a more complex

attractor, periodic or chaotic and located around x^*). Initial conditions out of the interval $[0, 1]$ generate sequences diverging to (minus) infinity. The boundary that separates the basin of attraction $\mathcal{B}(A)$ of the attractor A , from the basin $\mathcal{B}(\infty)$ is formed by the unstable fixed point $q^* = 0$ and its rank-1 preimage (different from itself), $q_{-1}^* = 1$. Observe that, of course, a fixed point is always preimage of itself, but in this case also another preimage exists because $q^* \in Z_2$. If $\mu < 4$, like in fig. 5a, $q_{-1}^* > c = \mu/4$, where c is the critical point (maximum) that separates Z_0 and Z_2 . Hence, $q_{-1}^* \in Z_0$. If we increase μ , at $\mu = 4$ we have $q_{-1}^* = c = 1$, and a contact between the critical point and the basin boundary occurs. This is a global bifurcation, which changes the structure of the basin. For $\mu > 4$, we have $q_{-1}^* < c$, and the portion (q_{-1}^*, c) of $\mathcal{B}(\infty)$ enters Z_2 . This implies that new preimages of that portion are created, which belong to $\mathcal{B}(\infty)$ according to (4). The two rank-1 preimages of (q_{-1}^*, c) are located in a neighborhood I_0 of the critical point $c_{-1} = 1/2$, as shown in fig. 5b. Points of I_0 exit the interval $(0, 1)$ after one iteration, thus giving an unbounded sequence. As $I_0 \in Z_2$, it also has two rank-1 preimages, that are rank-2 preimages of (q_{-1}^*, c) . These preimages are given by the two smaller intervals denoted by $I_{-1}^{(1)}$ and $I_{-1}^{(2)}$ in fig. 5b and are located symmetrically with respect to $c_{-1} = 1/2$. Points belonging to $I_{-1}^{(1)}$ and $I_{-1}^{(2)}$ exit the interval $(0, 1)$ after two iterations of (5). Even these two smaller – non-connected – portions of $\mathcal{B}(\infty)$ are in Z_2 . Hence, each of them has two preimages, which again result in non-connected portions of $\mathcal{B}(\infty)$. Obviously, this process gives rise to a infinite sequence of preimages whose points generate unbounded sequences. So, after the contact between the critical point c and the basin boundary q_{-1}^* , infinitely many non-connected portions of $\mathcal{B}(\infty)$ are created inside $(0, 1)$ (only a few of them are shown in fig. 5b). The union of all these preimages is an open set whose closure is $[0, 1]$. Its complement in $[0, 1]$ has zero Lebesgue measure and is a Cantor set (see Guckenheimer and Holmes, [19], Devaney, [17]).

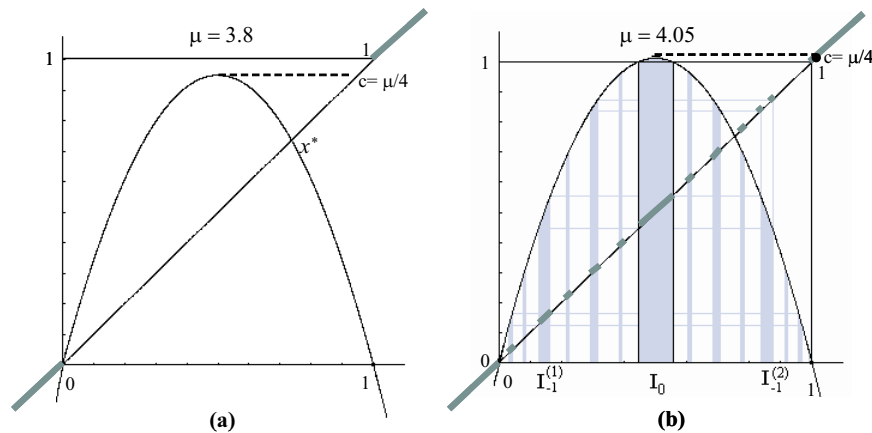


Figure 5

A similar situation occurs for a unimodal $Z_0 - Z_2$ map where the attractor at infinity is replaced by an attracting fixed point, like the one shown in fig. 6. As in the previous example, we have an attractor A , which may be the fixed point x^* (or some other invariant set around it), with a simply connected basin bounded by the unstable fixed point q^* and its rank-1 preimage q_{-1}^* . This example differs with respect to the previous one in so far as in this case initial conditions taken in the complementary set generate trajectories converging to the stable fixed point z^* . This means that the basin $\mathcal{B}(z^*)$ is formed by the union of two non-connected portions: $B_0 = (-\infty, q^*) \subset Z_2$, which contains z^* (usually called *immediate basin*, the largest connected component of the basin which contains the attractor) and $B_1 = (q_{-1}^*, +\infty) = f^{-1}(B_0) \subset Z_0$. In fig. 6 the two non-connected portions of the basin $\mathcal{B}(z^*)$ are marked by bold lines. Interesting effects occur, if some parameter variation causes an increase of the critical point c (maximum value) until it crosses the basin boundary q^* . If this happens, the interval (q_{-1}^*, c) , which is part of B_1 , enters Z_2 , and infinitely many non-connected portions of $\mathcal{B}(z^*)$ emerge in the interval (q^*, q_{-1}^*) . Note that the total basin can still be expressed as the union of all the preimages of any rank of the immediate basin B_0 .

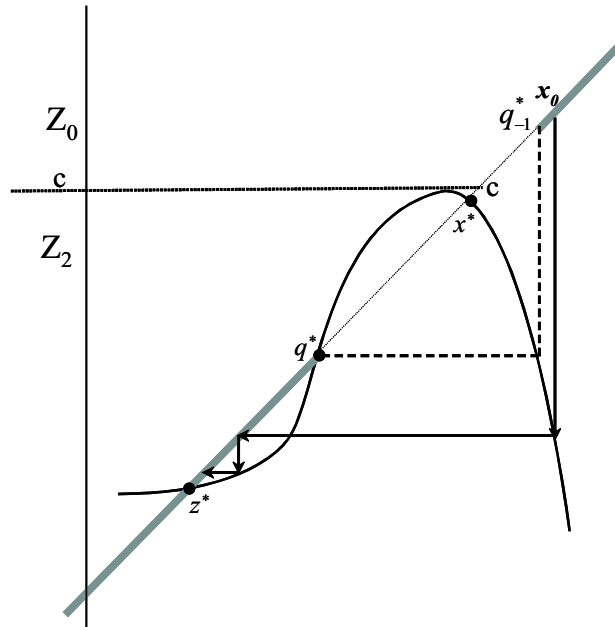


Figure 6

Another interesting situation is obtained if we change the right branch of the map of fig. 6 by folding it upwards such that another critical point, a minimum, is created. Such a situation is shown in fig. 7. This is a noninvertible $Z_1 - Z_3 - Z_1$ map, where Z_3 is the portion of the codomain bounded by the relative minimum value c_{\min} and relative maximum value c_{\max} . In the situation shown in fig. 7a we have three attractors: the fixed point z^* , with $\mathcal{B}(z^*) = (-\infty, q^*)$, the attractor A around x^* , with basin $\mathcal{B}(A) = (q^*, r^*)$ bounded by two unstable fixed points, and $+\infty$ (i.e. positively diverging trajectories) with basin $\mathcal{B}(+\infty) = (r^*, +\infty)$. In this case all the basins are immediate basins, each being given by an open interval. In the situation shown in fig. 7a, both basin boundaries q^* and r^* are in Z_1 , so they have only themselves as unique preimages (like for an invertible map). However, the situation drastically changes if, for example, some parameter changes causes the minimum value c_{\min} to move downwards, until it goes below q^* (as in fig. 7b). After the global bifurcation, when $c_{\min} = q^*$, the portion (c_{\min}, q^*) enters Z_3 , so new preimages $f^{-k}(c_{\min}, q^*)$ appear with $k \geq 1$. These preimages constitute non-connected portions of $\mathcal{B}(z^*)$ nested inside $\mathcal{B}(A)$, and are represented by the thick portions of the diagonal in fig. 7b.

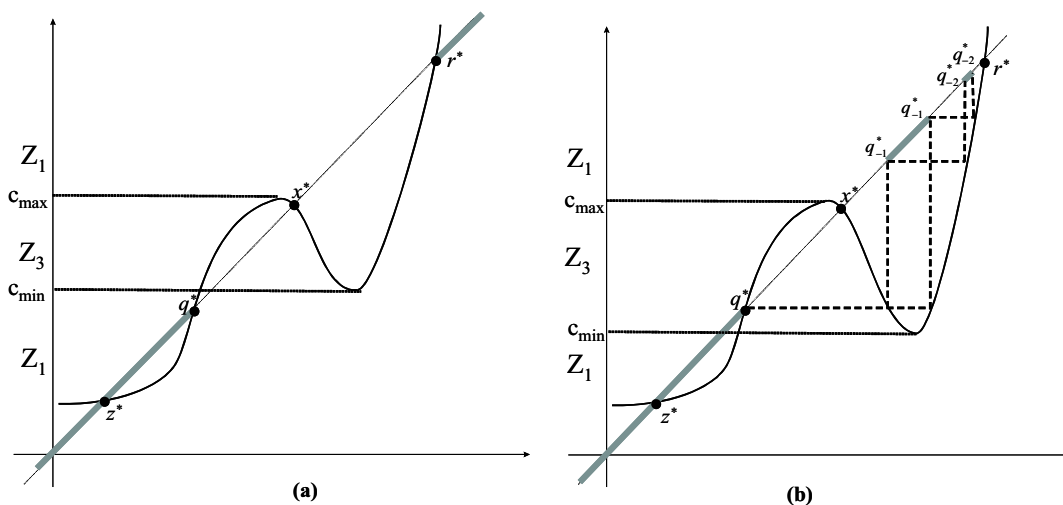


Figure 7

4 Two-Dimensional Dynamics

We now consider two examples, which are taken from recently published papers. In these models two-dimensional iterated maps are used to describe the time evolutions of players' actions in discrete time dynamic games. In each example we emphasize the creation of non-connected basins and how it can be explained in terms of contacts between critical curves and basin boundaries, where the latter are often formed by stable sets of saddle points or cycles. The first example is taken from Bischi and Kopel [7], who propose a dynamic duopoly game in the tradition of Cournot. In contrast to the early models on oligopoly dynamics, in their model players form adaptive expectations and players' reaction functions are unimodal. This framework gives rise to a situation of multistability, where the basins of each stable Nash equilibrium is a rather complicated set. The second example presents a dynamic brand competition model proposed by Bischi, Gardini and Kopel [9]. In this game a unique and stable fixed point exists, but the basin of the fixed point can have a very complicated structure.

4.1 Example 1: Quantity-setting duopoly games with adaptive expectations

The first example we present is a dynamic Cournot duopoly game with unimodal reaction functions. The two quantity-setting firms produce homogeneous goods and, since they do not know the competitor's output, they try to predict this quantity using an adaptive scheme. Let $x_1(t)$ and $x_2(t)$ be the outputs at time period t . The two players determine their production quantities of the next period, $x_1(t+1)$ and $x_2(t+1)$, by solving the optimization problems

$$\max_{x_1} \Pi_1(x_1, x_2^e(t+1)); \max_{x_2} \Pi_2(x_1^e(t+1), x_2) \quad (7)$$

where Π_i is the profit of player i , and $x_i^e(t+1)$, $i = 1, 2$ represent the predictions for the output of the competitor. The solutions of the optimization problems (assumed to be unique) are denoted by

$$\begin{aligned} x_1(t+1) &= r_1(x_2^e(t+1)) \\ x_2(t+1) &= r_2(x_1^e(t+1)) \end{aligned} \quad (8)$$

where r_1 and r_2 are called the *Best Replies* (or reaction functions). In the original work of Cournot [15], as well as in much of the literature which followed, *naive expectations* $x_i^e(t+1) = x_i(t)$ have been considered. Under the assumption of naive expectations each firm expects or predicts that the quantity offered by the competitor in the next period will be the same as in the current period. The time evolution of the duopoly system is then

represented by the two-dimensional discrete dynamical system

$$(x_1(t+1), x_2(t+1)) = (r_1(x_2(t)), r_2(x_1(t))) \quad (9)$$

which is also referred to as the *Cournot tâtonnement process*. In contrast to this, in Bischi and Kopel [7] firms are assumed to revise their beliefs according to the adaptive expectations scheme

$$\begin{aligned} x_1^e(t+1) &= x_1^e(t) + \alpha_1(x_1(t) - x_1^e(t)) \\ x_2^e(t+1) &= x_2^e(t) + \alpha_2(x_2(t) - x_2^e(t)) \end{aligned} \quad (10)$$

If the relations (8) are inserted into (10), one gets the following two-dimensional dynamical system in the belief space

$$\begin{aligned} x_1^e(t+1) &= (1 - \alpha_1)x_1^e(t) + \alpha_1 r_1(x_2^e(t)) \\ x_2^e(t+1) &= (1 - \alpha_2)x_2^e(t) + \alpha_2 r_2(x_1^e(t)) \end{aligned} \quad (11)$$

Of course, the quantities chosen by the competitors can be obtained by the transformations $x_1(t) = r_1(x_2^e(t))$, $x_2(t) = r_2(x_1^e(t))$, i.e. by a mapping from the belief space into the action space. The steady states of the dynamical system (11), defined by $x_i^e(t+1) = x_i^e(t)$, $i = 1, 2$, i.e.

$$\begin{aligned} x_1^e(t) &= r_1(x_2^e(t)) \\ x_2^e(t) &= r_2(x_1^e(t)) \end{aligned} \quad (12)$$

are located at the intersections of the two reaction curves and are independent of the adjustment coefficients α_1 and α_2 . In other words, a steady state is a situation where beliefs are not further revised and quantities do not change, and at the steady states the expected outputs coincide with the realized ones. Hence, in belief space we are considering a situation where beliefs are consistent and this corresponds to a Nash equilibrium in the quantity space. In Bischi and Kopel [7] the following reaction functions have been considered

$$\begin{aligned} r_1(x_2) &= \mu_1 x_2 (1 - x_2) \\ r_2(x_1) &= \mu_2 x_1 (1 - x_1) \end{aligned} \quad (13)$$

It has been shown elsewhere (see Kopel, [21]) that if the competitors regard their products as strategic complements over a certain range of the set of admissible actions, the functions given in (13) can be derived as Best Responses, and the parameters μ_i , $i = 1, 2$ measure the intensity of the positive externality the actions of one player exert on the payoff of the other player.

To simplify the notation, we rename the expected outputs by setting $x(t) = x_1^e(t)$ and $y(t) = x_2^e(t)$. Inserting the reaction functions specified in (13) into (11), the time evolution of the competitors' beliefs is obtained by the iteration of the two-dimensional map $T : (x, y) \rightarrow (x', y')$ defined by

$$\begin{aligned} x' &= (1 - \alpha_1)x + \alpha_1 \mu_1 y (1 - y) \\ y' &= (1 - \alpha_2)y + \alpha_2 \mu_2 x (1 - x) \end{aligned} \quad (14)$$

Under the assumption $\mu_1 = \mu_2 = \mu$, the fixed points can be expressed by simple analytical expressions: besides the trivial solution $O = (0, 0)$, a positive symmetric equilibrium exists for $\mu > 1$, given by $S = ((\mu - 1)/\mu, (\mu - 1)/\mu)$. Two further equilibria $E_1 = (\bar{x}, \bar{y})$ and $E_2 = (\bar{y}, \bar{x})$ exist for $\mu > 3$, where $\bar{x} = (\mu + 1 + \sqrt{\psi})/2\mu$, $\bar{y} = (\mu + 1 - \sqrt{\psi})/2\mu$ with $\psi = (\mu + 1)(\mu - 3)$. These equilibria are located in symmetric positions with respect to the diagonal Δ . The corresponding Nash equilibria have the same entries. As shown in Bischi and Kopel [7], a wide range of parameters μ, α_1, α_2 exists such that E_1 and E_2 are both stable. Accordingly, a problem of equilibrium selection arises, which leads to the question of the delimitation of the two basins of attraction $\mathcal{B}(E_1)$ and $\mathcal{B}(E_2)$.

As argued in the previous sections, the properties of the inverses of the map become important in order to understand the structure of the basins and their qualitative changes. The map (14) is a noninvertible map. This can be deduced from the fact that given a point $(x', y') \in \mathbb{R}^2$, its rank-1 preimages may be up to four; they can be computed by solving the fourth degree algebraic system (14) with respect to x and y . The critical curves are computed as follows: LC_{-1} coincides with the set of points in which the Jacobian determinant vanishes, i.e. $\det DT = 0$, where

$$DT(x, y) = \begin{bmatrix} 1 - \alpha_1 & \alpha_1 \mu_1 (1 - 2y) \\ \alpha_2 \mu_2 (1 - 2x) & 1 - \alpha_2 \end{bmatrix} \quad (15)$$

and $LC = T(LC_{-1})$. So, LC_{-1} is an equilateral hyperbola, of equation

$$\left(x - \frac{1}{2}\right) \left(y - \frac{1}{2}\right) = \frac{(1 - \alpha_1)(1 - \alpha_2)}{4\alpha_1\alpha_2\mu_1\mu_2}. \quad (16)$$

Since LC_{-1} is formed by the union of two disjoint branches, say $LC_{-1} = LC_{-1}^{(a)} \cup LC_{-1}^{(b)}$, it follows that also $LC = T(LC_{-1})$ is the union of two branches, say $LC^{(a)} = T(LC_{-1}^{(a)})$ and $LC^{(b)} = T(LC_{-1}^{(b)})$, see figs. 8a and 8b. The branch $LC^{(a)}$ separates the region Z_0 , whose points have no preimages, from the region Z_2 , whose points have two distinct rank-1 preimages. The other branch $LC^{(b)}$ separates the region Z_2 from Z_4 , whose points have four distinct preimages. Any point of $LC^{(a)}$ has two coincident rank-1 preimages, located at a point of $LC_{-1}^{(a)}$, and any point of $LC^{(b)}$ has two coincident rank-1 preimages, located at a point of $LC_{-1}^{(b)}$, plus two further distinct rank-1 preimages, called *extra preimages*. Following the terminology of Mira et al. [24], we say that the map (14) is a noninvertible map of $Z_4 > Z_2 - Z_0$ type, where the symbol “>” denotes the presence of a cusp point in the branch $LC^{(b)}$ (see fig. 8b). The corresponding *Riemann foliation* is shown in fig. 8c. Different sheets are connected by folds joining two sheets, and the projections of such folds on the phase plane are arcs of LC . The cusp point of LC is characterized by three merging preimages at the junction of two folds.

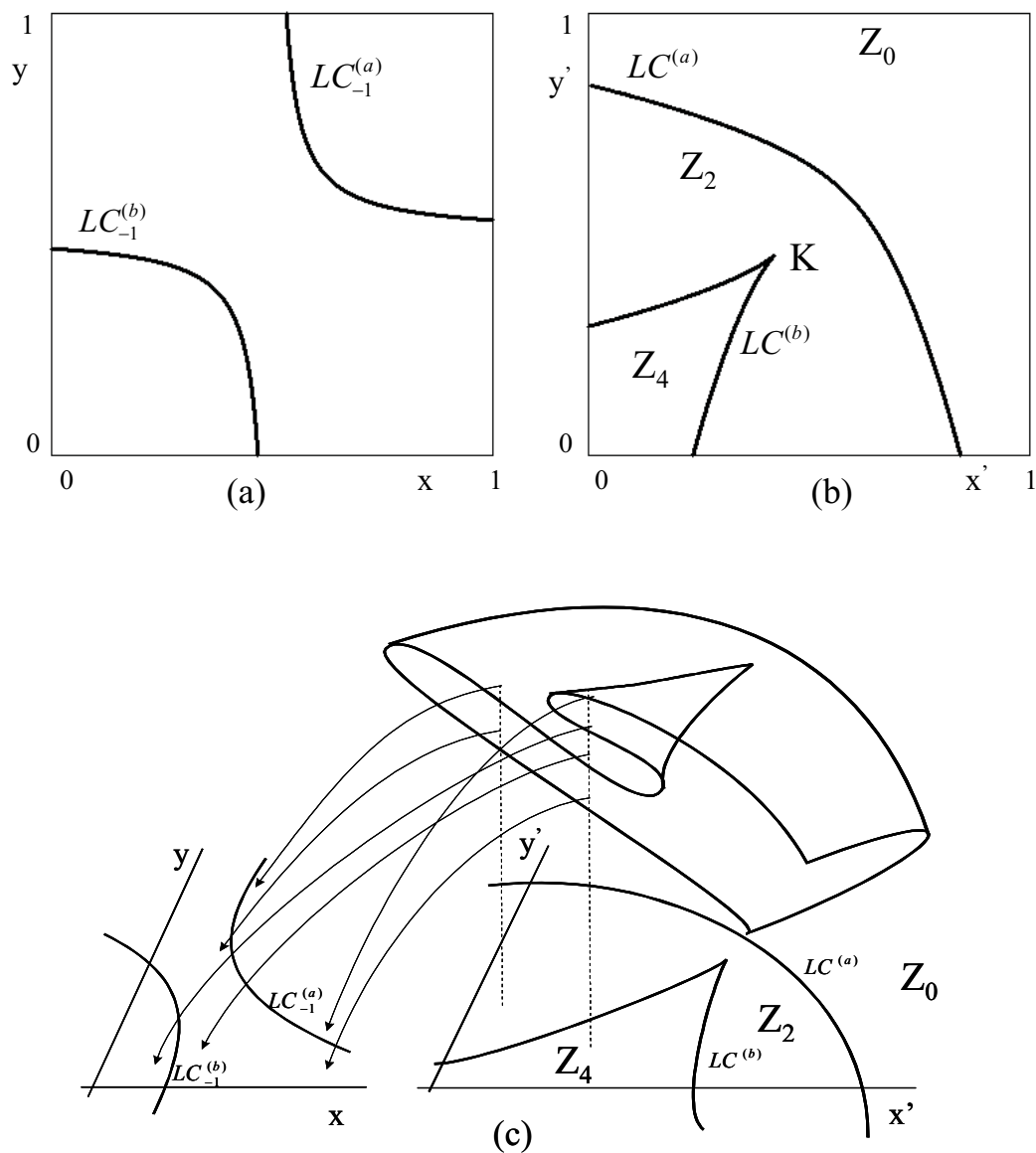


Figure 8

In order to study the structure of the basins and explain the global bifurcations that change their qualitative properties, we first consider the symmetric case of players with homogeneous expectations, i.e. $\alpha_1 = \alpha_2 = \alpha$. In this case, the map (14) has a symmetry

property, as it remains the same if the variables x and y are swapped. Formally, we have $T(P(x, y)) = P(T(x, y))$, where $P : (x, y) \rightarrow (y, x)$ is the reflection through the diagonal $\Delta = \{(x, x), x \in \mathbb{R}\}$. This symmetry property implies that the diagonal Δ is a trapping subspace for the map T , i.e. $T(\Delta) \subseteq \Delta$. The trajectories embedded in Δ are governed by the restriction of the two-dimensional map T to Δ , i.e. $f = T|_{\Delta} : \Delta \rightarrow \Delta$. The map f , obtained by setting $x = y$ and $x' = y'$ in (14), is given by $x' = f(x) = (1 + \alpha(\mu - 1))x - \alpha\mu x^2$. In the symmetric case of homogeneous players we can give a complete analytical characterization of the global bifurcation that transforms the basins from simply connected sets to multiply connected. In fact, the following result is given in Bischi and Kopel [7]:

If $\mu_1 = \mu_2 = \mu$ and $\alpha_1 = \alpha_2 = \alpha$ and the equilibria E_1 and E_2 are both stable, then the common boundary $\partial\mathcal{B}(E_1) \cap \partial\mathcal{B}(E_2)$ which separates the basin $\mathcal{B}(E_1)$ from the basin $\mathcal{B}(E_2)$ is given by the stable set $W^s(S)$ of the saddle point S . If $\alpha(\mu + 1) < 1$ then $W^s(S) = OO_{-1}^{(1)}$, where $O = (0, 0)$ and $O_{-1}^{(1)} = \left(\frac{1+\alpha(\mu-1)}{\alpha\mu}, \frac{1+\alpha(\mu-1)}{\alpha\mu}\right)$, and the two basins are simply connected sets. If $\alpha(\mu + 1) > 1$ then the two basins are non-connected sets, formed by infinitely many simply connected components.

The bifurcation occurring at $\alpha(\mu + 1) = 1$ is a *global bifurcation*. It cannot be revealed by a study of the linear approximation of the dynamical system and the occurrence of such a bifurcation can be characterized by a contact between the stable set of the symmetric fixed point S and a critical curve. In order to explain this, we start from a set of parameters such that both of the basins are simply connected, like in fig. 9a, where $\mu_1 = \mu_2 = \mu = 3.4$ and $\alpha_1 = \alpha_2 = \alpha = 0.2 < 1/(\mu + 1)$. For this set of parameters, four fixed points exist, indicated by O , S , E_1 and E_2 . The fixed points O and S are saddle points, whereas the Nash equilibria E_1 and E_2 are both stable, each with its own basin of attraction. These basins, $\mathcal{B}(E_1)$ and $\mathcal{B}(E_2)$, are represented by white and light grey respectively (the dark grey region represents the set of initial conditions which generate unbounded trajectories; we could refer to this set as the basin of infinity). In this situation, any bounded trajectory starting with $x_1^e(0) > x_2^e(0)$ ($x_1^e(0) < x_2^e(0)$) converges to E_1 (E_2). In economic terms this means that an initial difference in the expectations of the competitors uniquely determines which of the equilibria is selected in the long run. Expectations of the players become self-fulfilling: if $x_1^e(0) > x_2^e(0)$ ($x_1^e(0) < x_2^e(0)$) then $x_1^e(t) > x_2^e(t)$ ($x_1^e(t) < x_2^e(t)$) for any t and equilibrium E_1 , where firm 1 dominates the market (equilibrium E_2 at which firm 2 dominates the market) is selected in the long run. In contrast to this, the situation shown in fig. 9b, where the value of the parameter μ is the same, but $\alpha_1 = \alpha_2 = 0.5 > 1/(\mu + 1)$, is quite different. In fact, in this case the basins are no longer simply connected sets. Many portions of each basin are present, both in the region above and below the diagonal, and the adjustment process of our dynamic game starting with initial beliefs $x_1^e(0) > x_2^e(0)$ (or $x_1^e(0) < x_2^e(0)$) may lead to convergence to either of the equilibria.

Now let us turn to an explanation of the global bifurcation which causes the transition between these rather different structures of the basins. First notice that the boundary separating $\mathcal{B}(E_1)$ and $\mathcal{B}(E_2)$ contains the symmetric equilibrium S as well as its whole stable set $W^s(S)$. In fact, just after the creation of the two stable fixed points E_1 and E_2 for $\mu = 3$, the symmetric equilibrium $S \in \Delta$ is a saddle point. The two branches of the unstable set $W^u(S)$ departing from it reach E_1 and E_2 respectively. Hence, since a basin boundary is backward invariant (see Mira et al., [24], [22]), not only the local stable set $W_{loc}^s(S)$ belongs to the boundary that separates the two basins, but also its preimages of any rank: $W^s(S) = \bigcup_{k \geq 0} T^{-k}(W_{loc}^s(S))$. Because of the symmetry property of the system (14) with homogeneous players, the local stable set of S belongs to the invariant diagonal Δ . As long as $\alpha(\mu + 1) < 1$, the whole stable set $W^s(S)$ belongs to Δ and is given by $W^s(S) = OO_{-1}^{(1)}$, where $O_{-1}^{(1)}$ is the preimage of O located along Δ . Observe that if $\alpha(\mu + 1) < 1$ holds, the cusp point K of the critical curve $LC^{(b)}$ has negative coordinates and, consequently, the whole segment $OO_{-1}^{(1)}$ belongs to the regions Z_0 and Z_2 , see fig. 9a. This implies that the two preimages of any point of $OO_{-1}^{(1)}$ belong to Δ (they can be computed by the restriction f of T to the invariant diagonal Δ). This proves that the segment $OO_{-1}^{(1)}$ is backward invariant, i.e. it includes all its preimages. The structure of the basins $\mathcal{B}(E_i)$, $i = 1, 2$, is very simple: $\mathcal{B}(E_1)$ is entirely located below the diagonal Δ and $\mathcal{B}(E_2)$ is entirely located above it. Both of the basins $\mathcal{B}(E_1)$ and $\mathcal{B}(E_2)$ are simply connected sets.

Their structure becomes a lot more complex for $\alpha(\mu + 1) > 1$. In order to understand the bifurcation occurring at $\alpha(\mu + 1) = 1$, we consider the critical curves of the map (14). At $\alpha(\mu + 1) = 1$ a contact between $LC^{(b)}$ and the fixed point O occurs, due to the merging between O and the cusp point K .² For $\alpha(\mu + 1) > 1$, the portion KO of $W_{loc}^s(S)$ belongs to the region Z_4 , where four inverses of T exist. This implies that besides the two rank-1 preimages on Δ , the points of KO have two further preimages, which are located on the segment $O_{-1}^{(2)}O_{-1}^{(3)}$ of the line Δ_{-1} . Since $OO_{-1}^{(1)} = W_{loc}^s(S) \subset \partial\mathcal{B}(E_1) \cap \partial\mathcal{B}(E_2)$, also its preimages of any rank belong to the boundary which separates $\mathcal{B}(E_1)$ from $\mathcal{B}(E_2)$. So the rank-1 preimages of the segment $O_{-1}^{(2)}O_{-1}^{(3)}$, which exist because portions of it are included in the regions Z_2 and Z_4 , belong to $W^s(S)$ as well, being preimages of rank-2 of $OO_{-1}^{(1)}$. This repeated procedure, based on the iteration of the multi-valued inverse of T , leads to the construction of the whole stable set $W^s(S)$.

²To compute the coordinates of the cusp point of $LC^{(b)}$ notice that in any point of LC_{-1} at least one eigenvalue of DT vanishes. In the point $C_{-1} = LC_{-1}^{(a)} \cap \Delta = (c_{-1}, c_{-1})$, with $c_{-1} = (\alpha(\mu - 1) + 1)/2\alpha\mu$, the eigenvalue z_{\parallel} with eigendirection along Δ vanishes, and its image $C = LC^{(a)} \cap \Delta = (c, c)$ with $c = f(c_{-1}) = (\alpha(\mu - 1) + 1)^2/4\alpha\mu$ is the point at which $LC^{(a)}$ intersects Δ . This corresponds to the unique critical point of the restriction of T to Δ . At the other intersection of LC_{-1} with Δ , given by $K_{-1} = LC_{-1}^{(b)} \cap \Delta = (k_{-1}, k_{-1})$ with $k_{-1} = (\alpha(\mu - 1) - 1)/2\alpha\mu$ the eigenvalue z_{\perp} vanishes, and the curve $LC^{(b)} = T(LC_{-1}^{(b)})$ has a cusp point (see e.g. Arnold et al., 1986) $K = LC^{(b)} \cap \Delta = (k, k)$ with $k = f(k_{-1}) = (\alpha(\mu + 1) - 1)(\alpha\mu + 3(1 - \alpha))/4\alpha\mu$

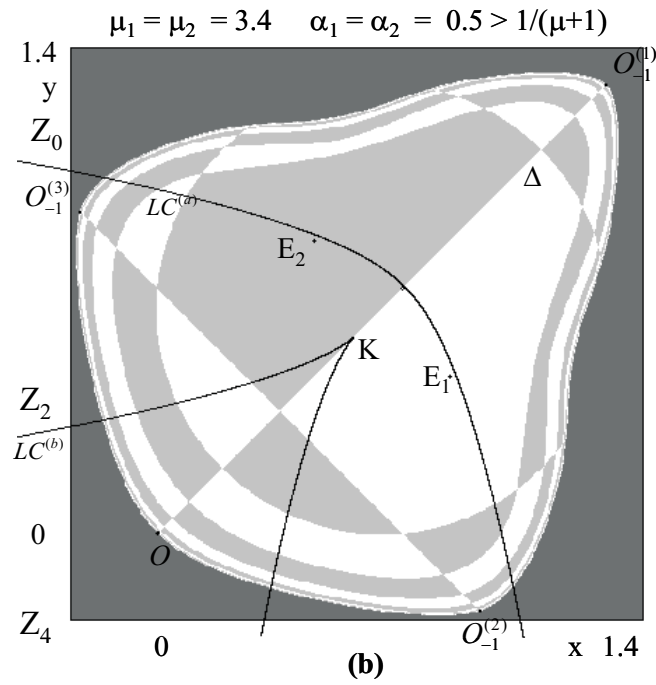
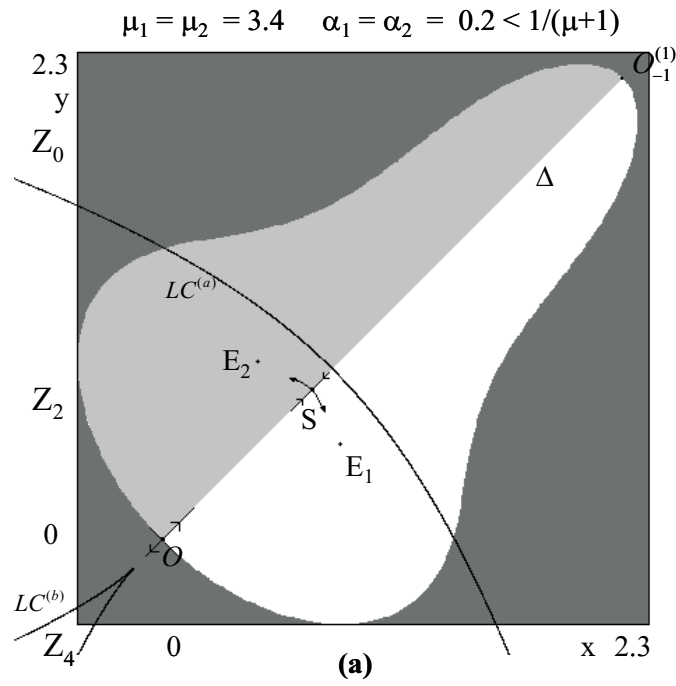


Figure 9

Similar results can be obtained in the case of heterogeneous players, where the heterogeneity arises e.g. due to different speeds of adjustment $\alpha_1 \neq \alpha_2$. The main difference with respect to the homogeneous case lies in the fact that the diagonal Δ is no longer invariant. Even if the fixed points remain the same, the basins are no longer symmetric with respect to Δ . Nevertheless, many of the arguments given above continue to hold in the case of heterogeneous beliefs. In particular, the boundary which separates the basin of equilibrium E_1 from that of E_2 is still formed by the whole stable set $W^s(S)$, but in the case $\alpha_1 \neq \alpha_2$ the local stable set $W_{loc}^s(S)$ is not along the diagonal Δ . The contact between $W^s(S)$ and $LC^{(b)}$, which causes the transition from simple to complex basins, does not occur at O (since now $O \notin W^s(S)$) and no longer involves the cusp point of $LC^{(b)}$. So, the parameter values at which such contact bifurcations occur cannot be computed analytically.

In fig. 10a, obtained with $\mu = 3.6$, $\alpha_1 = 0.55$ and $\alpha_2 = 0.7$, the two equilibria E_1 and E_2 are stable, and their basins are connected sets. An asymmetry in the expectation formation process has a negligible effect on the local stability properties of the equilibria, but it results in an evident asymmetry in the basins of attraction. As shown in fig. 10a, when $\alpha_2 > \alpha_1$ the extension of $\mathcal{B}(E_2)$ is, in general, greater than the extension of $\mathcal{B}(E_1)$.

Moreover, the situation is not always as simple as in fig. 10a. The symmetric equilibrium S is a saddle fixed point and is included in the boundary – the whole stable set $W^s(S)$ – which separates the two basins. It can be noticed that in the simple situation shown in fig. 10a, the whole stable set $W^s(S)$ is entirely included inside the regions Z_2 and Z_0 . However, the fact that a portion of $W^s(S)$ is close to LC suggests that a contact bifurcation may occur if, e.g., the adjustment coefficients are slightly changed. In fact, if a portion of $\mathcal{B}(E_1)$ enters Z_4 after a contact with $LC^{(b)}$, new rank-1 preimages of that portion will appear near $LC_{-1}^{(b)}$. This is the situation illustrated in fig. 10b, obtained after a small change of α_1 . The portion of $\mathcal{B}(E_1)$ inside Z_4 is denoted by H_0 . It has two rank-1 preimages, denoted by $H_{-1}^{(1)}$ and $H_{-1}^{(2)}$, which are located at opposite sides with respect to $LC_{-1}^{(b)}$ and merge on it (by definition the rank-1 preimages of the arc of $LC^{(b)}$ which bound H_0 must merge along $LC_{-1}^{(b)}$). The set $H_{-1} = H_{-1}^{(1)} \cup H_{-1}^{(2)}$ constitute a non-connected portion of $\mathcal{B}(E_1)$. Moreover, since H_{-1} belongs to the region Z_4 , it has four rank-1 preimages, denoted by $H_{-2}^{(j)}$, $j = 1, \dots, 4$ in fig. 10b, which constitute other four “islands”³ of $\mathcal{B}(E_1)$. Points of these “islands” are mapped into H_0 after two iterations of the map T . Indeed, infinitely many higher rank preimages of H_0 exist, thus giving infinitely many smaller and smaller disjoint “islands” of $\mathcal{B}(E_1)$. Hence, at the contact between $W^s(S)$ and LC , the basin $\mathcal{B}(E_1)$ is transformed from a simply connected into a non-connected set, constituted by infinitely many disjoint components. The larger connected component of $\mathcal{B}(E_1)$ which contains E_1 is the *immediate basin* $\mathcal{B}_0(E_1)$, and the whole basin is given by the union of the infinitely many

³We follow the terminology introduced in Mira et al. (1994).

preimages of $\mathcal{B}_0(E_1)$: $\mathcal{B}(E_1) = \bigcup_{k \geq 0} T^{-k}(\mathcal{B}_0(E_1))$. Observe that even if small differences between the adjustment speeds have negligible effects on the properties of the attractors, they may cause remarkable asymmetries in the structure of the basins, which can only be detected when the global properties of the economic model are studied.

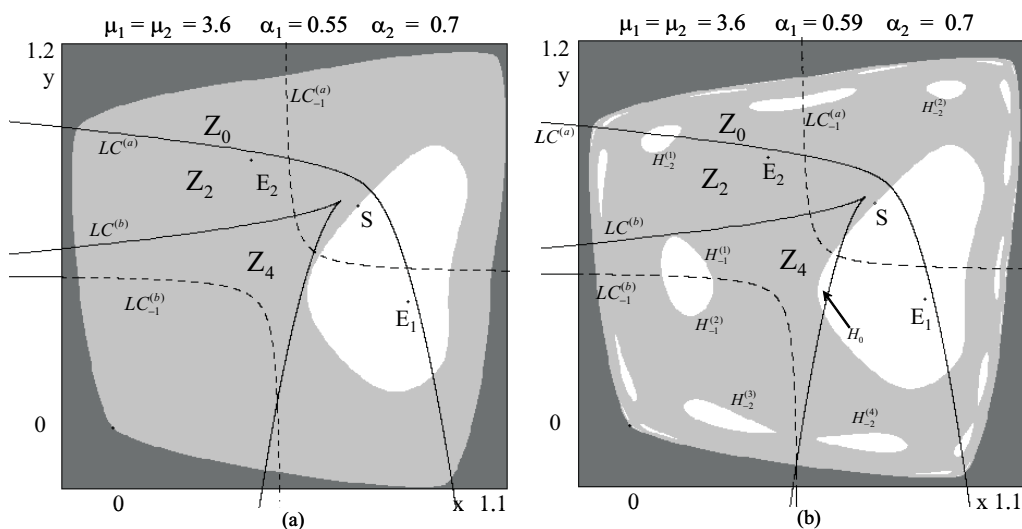


Figure 10

So, as in the one-dimensional case, the global bifurcation which causes a transformation of a basin from connected set into the union of infinitely many non-connected portions, is caused by a contact between a critical set and a basin boundary. However, since the equations of the curves involved in the contact often cannot be analytically expressed in terms of elementary functions, the occurrence of contact bifurcations can only be revealed numerically. This happens frequently in the study of nonlinear dynamical systems of dimension greater than one: results on global bifurcations are generally obtained through an interplay between theoretical and numerical methods, and the occurrence of these bifurcations is shown by computer-assisted proofs, based on the knowledge of the properties of the critical curves and their graphical representation (see e.g. Mira et al., [24], for many examples). This “modus operandi” is typical in the study of global bifurcations of nonlinear two-dimensional maps.

4.2 Example 2: A rent-seeking/competition game

The second dynamic model we present is used to describe a market game where a population of consumers can choose between two brands of homogeneous goods which are produced

by two competing firms. Let x_1 and x_2 represent the marketing efforts of two firms (e.g. advertising effort) and B the total sales potential of the market (in terms of customer market expenditures). If firm 1's effort is x_1 and firm 2's effort is x_2 , then the shares of the market (in terms of sales) accruing to firm 1 and to firm 2 are Bs_1 and $Bs_2 = B - Bs_1$, where

$$s_1 = \frac{ax_1^{\beta_1}}{ax_1^{\beta_1} + bx_2^{\beta_2}}, \quad s_2 = \frac{bx_2^{\beta_2}}{ax_1^{\beta_1} + bx_2^{\beta_2}}. \tag{17}$$

The terms $A_1 = ax_1^{\beta_1}$ and $A_2 = bx_2^{\beta_2}$ represent the recruitment of customers by firm 1 and 2, given the firms' efforts x_1 and x_2 . The parameters a and b denote the relative effectiveness of the effort made by the firms. Since $\frac{dA_1}{dx_1} \frac{x_1}{A_1} = \beta_1$ and $\frac{dA_2}{dx_2} \frac{x_2}{A_2} = \beta_2$, the parameters β_1 and β_2 denote the elasticities of the attraction of firm (or brand) i with regard to the effort of firm i . A dynamic model is obtained by assuming that the two competitors adjust their marketing efforts in response to the profits achieved in the previous period:

$$T : \begin{cases} x_1(t+1) = x_1(t) + \lambda_1 x_1(t) \left(B \frac{[x_1(t)]^{\beta_1}}{[x_1(t)]^{\beta_1} + k[x_2(t)]^{\beta_2}} - x_1(t) \right) \\ x_2(t+1) = x_2(t) + \lambda_2 x_2(t) \left(B \frac{[x_2(t)]^{\beta_2}}{[x_1(t)]^{\beta_1} + k[x_2(t)]^{\beta_2}} - x_2(t) \right) \end{cases} \tag{18}$$

The parameters $\lambda_i > 0, i = 1, 2$, measure the rate of this adjustment and $k := b/a$.

An important feature of the map (18) is that the two coordinate axes are invariant lines, since $T(x_1, 0) = (x_1', 0)$ and $T(0, x_2) = (0, x_2')$. The dynamics of (18) along the axis $x_i = 0$ are governed by one-dimensional maps $x_j' = f_j(x_j)$, where f_j is the restriction of T to the corresponding axis. The map f_j is given by $f_j(x_j) = (1 + \lambda_j B)x_j - \lambda_j x_j^2$. It is conjugate to the standard logistic map (5) by the homeomorphisms $x_j = x(1 + \lambda_j B)/\lambda_j$, where the parameters μ is given by $\mu = 1 + \lambda_j B$. Thus, the properties of the trajectories embedded in the invariant axes can be easily deduced from the well-known properties of the standard logistic map (5).

The fixed points of the map (18) are the solutions of the system

$$\begin{cases} x_1 \left(B \frac{x_1^{\beta_1}}{x_1^{\beta_1} + kx_2^{\beta_2}} - x_1 \right) = 0 \\ x_2 \left(B \frac{kx_2^{\beta_2}}{x_1^{\beta_1} + kx_2^{\beta_2}} - x_2 \right) = 0 \end{cases} \tag{19}$$

There are three evident "boundary solutions",

$$O = (0, 0); \quad E_1 = (B, 0); \quad E_2 = (0, B), \tag{20}$$

but O is not a fixed point because the map is not defined in it. The fixed points E_1 and E_2 are related to the positive fixed points of the one-dimensional quadratic maps f_1 and f_2 governing the dynamics along the invariant axes. There is also another fixed point, interior to the positive quadrant \mathbb{R}_+^2 , given by

$$E_* = (x_1^*, B - x_1^*). \tag{21}$$

The coordinate $x_1^* \in (0, B)$ is the unique solution of the equation $F(x) = k^{\frac{1}{1-\beta_2}} x^{\frac{1-\beta_1}{1-\beta_2}} + x - B = 0$, since F a continuous function with $F(0) < 0$, $F(B) > 0$ and $F'(x) > 0$ for each $x > 0$. With a given set of parameters B , β_1 and β_2 , the positive fixed point E_* is locally asymptotically stable for sufficiently small values of the adjustment speeds λ_1 and λ_2 . It loses stability as one or both of the adjustment speeds are increased and more complex attractors are created around it.

In the following we focus our attention on the global properties of the map (18), in particular on the boundaries of the *feasible set* \mathcal{B} . This feasible set is defined as the set of points which generate trajectories which are entirely in the positive orthant (feasible trajectories). A feasible trajectory may converge to the positive steady state E_* , to other more complex attractors inside \mathcal{B} or to a one-dimensional invariant set embedded inside a coordinate axis (the last occurrence means that one of the two brands disappears). Trajectories starting outside of the set \mathcal{B} represent infeasible evolutions of the economic system. As proved in Bischi, Gardini and Kopel [9], (18) is a noninvertible map of $Z_4 > Z_2 - Z_0$, and the qualitative shape of the critical curves, as well as the Riemann foliation, are similar to the ones of the previous example, see fig. 8. As before, starting from the knowledge of the global properties of the map (18), we illustrate how the boundaries of the feasible set changes when a structural parameter of the game is changed. By using the method of critical curves, we try to reveal the mechanism which is responsible for these changes.

With values of the parameters β_i in the range (0.2, 0.3), our numerical investigation has shown that the invariant coordinate axes are transversely repelling, i.e. they act as repelling sets with respect to trajectories approaching them from the interior of the nonnegative orthant. Moreover, for the parameters used in our simulations, we have observed only one attractor inside \mathcal{B} , although more than one coexisting attractors may exist, each with its own basin of attraction. On the basis of this numerical evidence, in what follows we will often speak of a unique bounded and positive attracting set \mathcal{A} , which attracts the generic feasible trajectory, even if its existence and uniqueness are not rigorously proved. Let $\partial\mathcal{B}$ be the boundary of \mathcal{B} . Such a boundary can have a simple shape, as in the situation shown in fig. 11a, where the attractor \mathcal{A} is the fixed point E_* and \mathcal{B} is represented by the white region. However, the basin can also have a very complex structure, as in fig. 12b, where, again, \mathcal{B} is given by the white points and \mathcal{A} is a chaotic attractor represented by the black points inside \mathcal{B} .

An exact determination of $\partial\mathcal{B}$ is the main goal of the remainder of this subsection. Let us first consider the dynamics of T restricted to the invariant axes. We know that the maps f_j that govern the dynamics along the invariant axes are conjugated to the logistic map (5). This insight is important, and the reader is urged to recall the properties of this one-dimensional map, see section 3 and fig. 5. For $\lambda_1 B \leq 3$ (corresponding to $\mu \leq 4$), we can deduce that bounded trajectories along the x_1 axis are obtained, as long as the initial conditions are taken inside the segment $\omega_1 = OO_{-1}^{(1)}$. The point $O_{-1}^{(1)}$ is the rank-1 preimage

of the origin O computed for the one-dimensional restriction f_1 (see fig. 11a), i.e.

$$O_{-1}^{(1)} = \left(\frac{1 + \lambda_1 B}{\lambda_1}, 0 \right). \tag{22}$$

Divergent trajectories along the x_1 axis are obtained starting from an initial condition out of the segment ω_1 . Analogously, when $\lambda_2 B \leq 3$, bounded trajectories along the invariant x_2 axis are obtained provided that the initial conditions are taken inside the segment $\omega_2 = OO_{-1}^{(2)}$. In this case the point $O_{-1}^{(2)}$ is the rank-1 preimage of the origin computed for the restriction f_2 , i.e.

$$O_{-1}^{(2)} = \left(0, \frac{1 + \lambda_2 B}{\lambda_2} \right). \tag{23}$$

Divergent trajectories along the x_2 axis are obtained starting from an initial condition out of the segment ω_2 . Consider now the region bounded by the segments ω_1 and ω_2 and their rank-1 preimages $\omega_1^{-1} = T^{-1}(\omega_1)$ and $\omega_2^{-1} = T^{-1}(\omega_2)$. Such preimages can be analytically computed as follows. Let $X = (p, 0)$ be a point of ω_1 , i.e. $0 < p < \frac{1 + \lambda_1 B}{\lambda_1}$. Its preimages are the real solutions of the algebraic system obtained from (18) with $(x'_1, x'_2) = (p, 0)$:

$$\begin{cases} x_1 \left(1 + \lambda_1 B \frac{x_1^{\beta_1}}{x_1^{\beta_1} + kx_2^{\beta_2}} - \lambda_1 x_1 \right) = p \\ x_2 \left(1 + \lambda_2 B \frac{kx_2^{\beta_2}}{x_1^{\beta_1} + kx_2^{\beta_2}} - \lambda_2 x_2 \right) = 0 \end{cases} \tag{24}$$

It is easy to see that the preimages of the point X are either located on the same invariant axis $x_2 = 0$ (in the points whose coordinates are the solutions of the equation $f_1(x_1) = p$) or on the curve of equation

$$x_1 = \left[kx_2^{\beta_2} \left(\frac{\lambda_2 B - \lambda_2 x_2 + 1}{\lambda_2 x_2 - 1} \right) \right]^{\frac{1}{\beta_1}}. \tag{25}$$

Analogously, the preimages of a point $Y = (0, q)$ of ω_2 , i.e. $0 < q < \frac{1 + \lambda_2 B}{\lambda_2}$, belong to the same invariant axis $x_1 = 0$ (in the points whose coordinates are the solutions of the equation $f_2(x_2) = q$), or lie on the curve of equation

$$x_2 = \left[\frac{x_1^{\beta_1}}{k} \left(\frac{\lambda_1 B - \lambda_1 x_1 + 1}{\lambda_1 x_1 - 1} \right) \right]^{\frac{1}{\beta_2}}. \tag{26}$$

It is straightforward to see that the curve (25) intersects the x_2 axis in the point $O_{-1}^{(2)}$ given in (23), the curve (26) intersects the x_1 axis in the point $O_{-1}^{(1)}$ given in (22), and the two curves (25) and (26) intersect at a point $O_{-1}^{(3)}$ interior to the positive orthant (see fig. 11a). The point $O_{-1}^{(3)}$ is another rank-1 preimage of the origin. The four preimages of the origin are the vertexes of a “quadrilateral” $OO_{-1}^{(1)}O_{-1}^{(3)}O_{-1}^{(2)}$, whose sides are ω_1 , ω_2 and their rank-1

preimages ω_1^{-1} and ω_2^{-1} , which are located on the curves of equation (25) and (26). All the points outside this quadrilateral cannot generate feasible trajectories. In fact, points located on the right of ω_2^{-1} are mapped into points with negative x_1 coordinate after one iteration, as can be easily deduced from the first line of (18). Points located above ω_1^{-1} are mapped into points with negative x_2 coordinate after one iteration, as can be deduced from the second line of (18).

The boundary of \mathcal{B} is given, in general, by the union of all preimages (of any rank) of the segments ω_1 and ω_2 :

$$\partial\mathcal{B}(\infty) = \left(\bigcup_{n=0}^{\infty} T^{-n}(\omega_1)\right) \cup \left(\bigcup_{n=0}^{\infty} T^{-n}(\omega_2)\right). \tag{27}$$

As long as $\lambda_1 B \leq 3$ and $\lambda_2 B \leq 3$ the boundary of \mathcal{B} has the simple shape shown in fig. 11a, because no preimages of higher rank of ω_1 and ω_2 exist. This is due to the fact that ω_1^{-1} and ω_2^{-1} are entirely included inside the region Z_0 of the plane whose points have no preimages. The situation is different when the values of the parameters are such that some portions of these curves belong to the regions Z_2 or Z_4 whose points have two and four preimages respectively. In this case preimages of higher order of ω_1 and ω_2 exist, say ω_1^{-k} and ω_2^{-k} , which form new portions of $\partial\mathcal{B}$. Such preimages of ω_1 and ω_2 of rank $k > 1$ bound regions whose points are mapped out of the feasible set \mathcal{B} after k iterations. In such a case the shape of the boundary of \mathcal{B} becomes far more complex. This change is due to a global bifurcation that can be explained by using the critical curves.

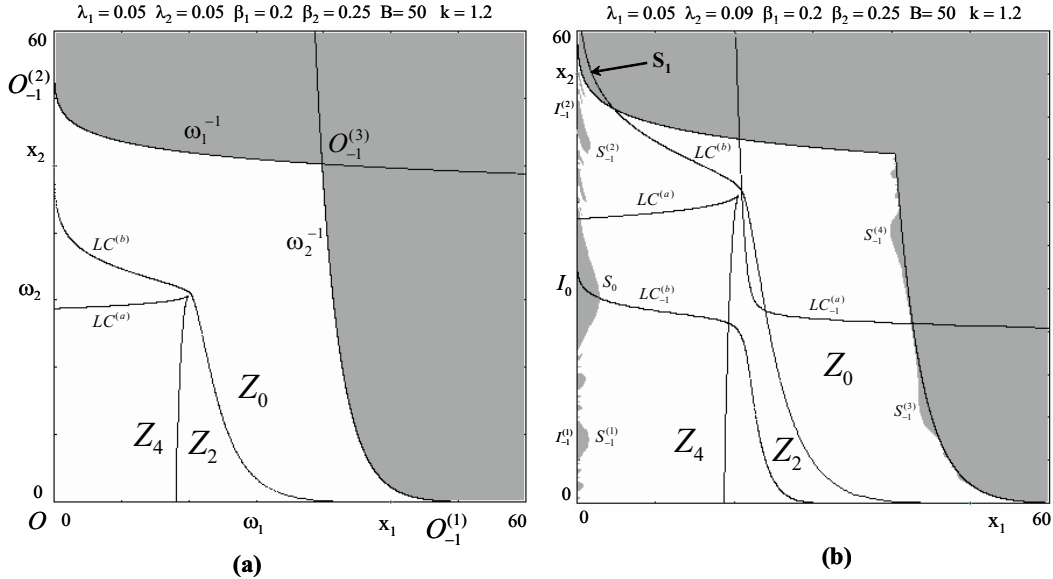


Figure 11

If λ_1 or λ_2 are increased so that the bifurcation value $\lambda_b = 3/B$ is crossed by at least one of them, then $\partial\mathcal{B}$ changes from smooth to fractal. To see this, we fix the parameters B, k, β_1, β_2 and λ_1 and vary the speed of adjustment λ_2 . As λ_2 is increased, the branch $LC^{(b)}$ of the critical curve that separates Z_0 from Z_2 moves upwards, and at $\lambda_2 = 3/B$ it has a contact with ω_1^{-1} at the point $O_{-1}^{(2)}$. After this contact, a segment of ω_1^{-1} enters the region Z_2 , so that a portion S_1 of the infeasible set, bounded by $LC^{(b)}$ and ω_1^{-1} , now has two preimages (see fig. 11b). These two preimages, say $S_0^{(1)}$ and $S_0^{(2)}$, merge in points of $LC_{-1}^{(b)}$ (as the points of $LC^{(b)}$ have two merging preimages belonging to $LC_{-1}^{(b)}$) and form a “grey tongue” issuing from the x_2 axis (denoted by S_0 in fig. 11b, with $S_0 = S_0^{(1)} \cup S_0^{(2)}$). S_0 belongs to the “grey set” of points that generate infeasible trajectories because the points of S_0 are mapped into S_1 , so that negative values are obtained after two iterations. Again, it is important to recall the fact that along the axes the dynamical behavior is governed by one-dimensional maps which are conjugate to the logistic map. We already know that the logistic map undergoes a global bifurcation at $\mu = 4$, where a contact between the critical point and the basin boundary occurs. This global bifurcation changes the structure of the basin for the one-dimensional map. A similar mechanism is at work here. To see this, look at the intersection of the “main tongue” S_0 with the x_2 axis. This gives a set I_0 around the critical point c_2 of the restriction f_2 . Of course, I_0 corresponds to the “main hole” of the logistic map with $\mu > 4$ (see fig. 5b). We know already, however, that I_0 has an infinite sequence of further preimages, $I_{-1}^{(1)}$ and $I_{-1}^{(2)}$, and so on. Accordingly, the set S_0 is only the first of infinitely many preimages of S_1 . Preimages of S_1 of higher rank form a sequence of smaller and smaller grey tongues issuing from the x_2 axis, whose intersection with the x_2 axis correspond to the infinitely many preimages I_{-k} of the main hole I_0 (see again fig. 5b). Only some of them are visible in fig. 11b, but smaller tongues become numerically visible by enlargements, as it usually happens with fractal curves. The fractal structure of the boundary of \mathcal{B} is a consequence of the fact that the tongues are distributed along the segment ω_2 of the x_2 axis according to the structure of the intervals I_{-k} described in section 3, whose complementary set is a Cantor set. In the situation shown in fig. 11b the main tongue S_0 has a wide portion in the region Z_4 . Hence, besides the two preimages along the x_2 axis (denoted by $S_{-1}^{(1)}$ and $S_{-1}^{(2)}$ in fig. 11b) issuing from the intervals $I_{-1}^{(1)}$ and $I_{-1}^{(2)}$, two more preimages exist. Hence, in the two-dimensional case the structure of the basin is even more complex. The additional preimages are denoted by $S_{-1}^{(3)}$ and $S_{-1}^{(4)}$ in fig. 11b, and are located at opposite sides with respect to $LC_{-1}^{(a)}$. The tongues $S_{-1}^{(3)}$ and $S_{-1}^{(4)}$ belong to Z_0 , hence they do not give rise to new sequences of tongues. On the other hand, $S_{-1}^{(1)}$ and $S_{-1}^{(2)}$ have further preimages, since they are located inside Z_4 and Z_2 respectively. If the preimages are two, as in the case of $S_{-1}^{(2)}$, they form two tongues issuing from the x_2 axis. In the case of four preimages, as in the case of $S_{-1}^{(1)}$, two of them are tongues issuing from the x_2 axis and two are tongues issuing from the opposite side, i.e. ω_2^{-1} .

As λ_2 is further increased, $LC^{(b)}$ moves upwards, the portion S_1 enlarges and, consequently, all its preimages (i.e. the infinitely many tongues) enlarge and become more pronounced. This causes the occurrence of another global bifurcation, that changes the set \mathcal{B} from simply connected to multiply connected (or connected with holes). The mechanism is similar to the one described in Mira et al. [24], [22] and Abraham et al. [1]. This second global bifurcation occurs when a tongue, belonging to Z_2 , has a contact with $LC^{(a)}$ and subsequently enters the region Z_4 . If such a contact occurs out of the x_2 axis, it causes the creation of a pair of new preimages. These preimages merge along $LC_{-1}^{(a)}$ and their union is a *hole* (or *lake*, following the terminology introduced in Mira et al. [22]) inside the feasible set \mathcal{B} . Accordingly, a set of points that generate infeasible trajectories has been created, and this set is surrounded by points of the feasible set \mathcal{B} . Such a situation is shown in fig. 12a, where a tongue has crossed $LC^{(a)}$ and the set H_1 is now in Z_4 . The hole H_0 of infeasible points is the preimage of the set H_1 , and is completely included in the feasible set. As λ_2 is further increased, other tongues cross $LC^{(a)}$ and, hence, new holes are created, giving a complicated structure of \mathcal{B} like the one shown in fig. 12b, where many holes inside \mathcal{B} are clearly visible.

To sum up, the transformation of the set \mathcal{B} from a simply connected region with smooth boundaries into a multiply connected set with fractal boundaries occurs through two types of global bifurcations, both due to contacts between $\partial\mathcal{B}$ and branches of the critical set LC . In fig. 12b it can be noticed that also the attractor inside \mathcal{B} changed its structure. For low values of λ_2 , as in fig. 11a, the attractor is the fixed point E_* , to which all the trajectories starting inside the set \mathcal{B} converge. As λ_2 increases, E_* loses stability through a flip (or period doubling) bifurcation, at which E_* becomes a saddle point, and an attracting cycle of period 2 is created near it. As λ_2 is further increased, a sequence of period doublings occurs, similar to the well-known Myrberg (or Feigenbaum) cascade for one-dimensional maps, which creates a sequence of attracting cycles of period 2^n followed by the creation of chaotic attractors, which may be cyclic chaotic sets or a connected chaotic set. So, both kinds of complexities can be observed in this model, even if there are no relations between them (for more details see Bischi, Gardini and Kopel, [9]).

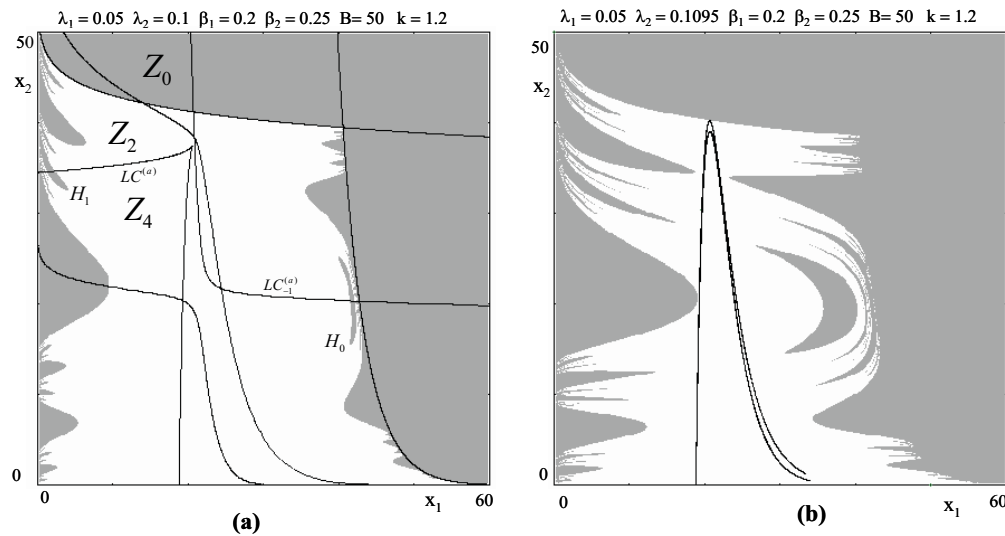


Figure 12

5 Conclusions

In this paper we have emphasized that there are two different routes to complexity. The literature on dynamic games has mainly focused on only one route. This route is related to the complexity of the attracting sets that characterize the long run evolution of the dynamic process and describe the evolution of players' actions over time. Unfortunately, it has neglected the second – for game theoretic considerations more important – route, namely the complexity of the boundaries which separate the basins when several coexisting attractors are present. As we have shown, these two kinds of complexity are *not related*, in the sense that complex attractors may have simple basins, whereas simple attractors like fixed points may have basins with very complex structure. We have used examples taken from the economics literature to illustrate how to perform a global analysis of a dynamic game. With the help of geometrical and numerical methods, the concepts of critical sets and basin boundaries, one can uncover the mechanism which gives rise to complex basins. During the last years, these tools have been used to analyze successfully the long run outcomes of dynamic economic models. Beside the papers we have mentioned above, there are applications in evolutionary game theory (Bischi et al., [12], [13]), fishery economics (Bischi and Kopel, [8], Bischi et al., [14]) and dynamic oligopoly games with three competitors (Agiza et al., [2], Bischi, Mroz and Hauser, [11]). It is our hope that with the present paper we have challenged the reader enough to join this dynamic game.

References

- [1] ABRAHAM, R., GARDINI, L. AND MIRA, C., *Chaos in discrete dynamical systems (a visual introduction in two dimensions)*, Springer, 1997.
- [2] AGIZA, H.N., BISCHI, G.I. AND KOPEL, M., *Multistability in a dynamic Cournot game with three oligopolists*, *Mathematics and Computers in Simulation* **51** (1999), pp. 63–90.
- [3] A. AGLIARI, G.I., BISCHI AND GARDINI, L., *Some methods for the Global Analysis of Dynamic Games represented by Noninvertible Maps*, Chapter 3 in *Oligopoly and Complex Dynamics: Tools & Models*, T. Puu and I. Sushko (eds.), Springer Verlag (in press).
- [4] ARNOLD, V., VARCHENKO, A. AND GOUSSEIN-ZADE, S., *Singularities des Applications Differentiables*, Editions MIR, Moscow, 1986.
- [5] BINMORE, K., *Fun and Games*, D.C. Heath & C., 1992.
- [6] BINMORE, K., Foreword to J.W. Weibull, *Evolutionary Game Theory*, The MIT Press, 1995.
- [7] BISCHI, G.I. AND KOPEL, M., *Equilibrium Selection in a Nonlinear Duopoly Game with Adaptive Expectations*, *Journal of Economic Behavior and Organization*, vol. 46/1, (2001), pp. 73–100.
- [8] BISCHI, G.I. AND KOPEL, M., *The Role of Competition, Expectations and Harvesting Costs in Commercial Fishing*, Chapter 4 in *Oligopoly and Complex Dynamics: Tools & Models*, T. Puu and I. Sushko editors, Springer Verlag (in press).
- [9] BISCHI, G.I., GARDINI, L. AND KOPEL, M., *Analysis of Global Bifurcations in a Market Share Attraction Model*, *Journal of Economic Dynamics and Control*, **24** (2000), pp. 855–879.
- [10] BISCHI, G.I., MAMMANA, C. AND GARDINI, L., *Multistability and cyclic attractors in duopoly games*, *Chaos, Solitons & Fractals*, **11** (2000), pp. 543–564.
- [11] BISCHI, G.I., MROZ, L. AND HAUSER, H., *Studying basin bifurcations in nonlinear triopoly games by using 3D visualization*, *Nonlinear Analysis, Theory, Methods and Applications*, vol. 47/8, (2001), pp. 5325–5341.
- [12] BISCHI, G.I., DAWID, H. AND KOPEL, M., *Spillover Effects and the Evolution of Firm Clusters*, *Journal of Economic Behavior and Organization* (in press).

- [13] BISCHI, G.I., DAWID, H. AND KOPEL, M., *Gaining the Competitive Edge Using Internal and External Spillovers: A Dynamic Analysis*, Journal of Economic Dynamics and Control, (in press).
- [14] BISCHI, G.I., KOPEL, M. AND SZIDAROVSKI, F., *Fishery dynamics under imperfect competition and adaptive expectations*, working paper, University of Arizona, USA, 2002.
- [15] COURNOT, A., *Researches into the principles of the theory of wealth*. Engl. transl., Chapter VII, 1963, Irwin Paperback Classics in Economics, 1838.
- [16] DANA, R.-A. AND MONTRUCCHIO, L., *Dynamic complexity in duopoly games*, Journal of Economic Theory, **40** (1986), pp. 40–56.
- [17] DEVANEY, R.L., *An Introduction to Chaotic Dynamical Systems*, The Benjamin/Cummings Publishing Co., Menlo Park, 1989.
- [18] FUDENBERG, D. AND LEVINE, D.K., *The Theory of Learning in Games*, MIT Press, Cambridge, Massachusetts, 1998.
- [19] GUCKENHEIMER, J. AND HOLMES, P., *Nonlinear Oscillations, Dynamical Systems and Bifurcations of Vector Fields*, Springer, 1983.
- [20] J. HOFBAUER AND SIGMUND, K., *Evolutionary Games and Population Dynamics*, Cambridge University Press, 1998.
- [21] KOPEL, M., *Simple and complex adjustment dynamics in Cournot Duopoly Models*, Chaos, Solitons, and Fractals, **7** (1996), pp. 2031–2048.
- [22] MIRA, C., FOURNIER-PRUNARET, D., GARDINI, L., KAWAKAMI, H. AND CATHALA, J.C., *Basin bifurcations of two-dimensional noninvertible maps: fractalization of basins*, International Journal of Bifurcations and Chaos, **4** (1994), pp. 343–381.
- [23] MIRA, C., CARCASSES, J.-P., MILLERIOUX, G. AND GARDINI, L., *Plane foliation of two-dimensional noninvertible maps*, Int. Jou. of Bif. & Chaos, vol.6 (8), (1996), pp. 1439–1462.
- [24] MIRA, C., GARDINI, L., BARUGOLA, A. AND CATHALA, J.C., *Chaotic Dynamics in Two-Dimensional Noninvertible Maps*, World Scientific, Singapore, 1996.
- [25] PUU, T., *Chaos in Duopoly Pricing*, Chaos, Solitons & Fractals, vol.1 n.6, (1991), pp. 573–581.
- [26] PUU, T., *The chaotic Duopolists revisited*, Journal of Economic Behavior and Organization, **33** (1998), pp. 385–394.

- [27] RAND, D., *Exotic phenomena in games and duopoly models*, Journal of Mathematical Economics, **5** (1978), pp. 173–184.
- [28] RASSENTI, S., REYNOLDS, S.S., SMITH, V.L. AND SZIDAROVSKY, F., *Adaptation and Convergence in Repeated Experimental Cournot Games*, Journal of Economic Behavior and Organization **41** (2000), pp. 117–146.
- [29] ROSSER JR., J.B., *Complex ecologic-economic dynamics and environmental policy*, Ecological Economics, (2001), pp. 23–37.
- [30] VAN HUYCK, J.B., COOK, J.P., AND BATTALIO, R.C., *Selection dynamics, asymptotic stability, and adaptive behavior*, Journal of Political Economy, **102** (1994), pp. 975–1005.
- [31] VAN WITTELOOSTUIJN, A. AND VAN LIER, A., *Chaotic patterns in Cournot competition*, Metroeconomica, **41** (1990), pp. 161–185.
- [32] J.W. WEIBULL, *Evolutionary Game Theory*, The MIT Press, 1995.